

### Microscopic screening and phonon dispersion in germanium

P. E. Van Camp, V. E. Van Doren, and J. T. Devreese\*

Rijksuniversitair Centrum Antwerpen, Groenenborgerlaan 171, B-2020 Antwerpen, Belgium

(Received 2 January 1979)

This paper shows results for the phonon dispersion of Ge in an extreme-tight-binding calculation for different values of the ionic-pseudopotential parameters. It is found that in this model meaningful results, comparable to experiment, can be obtained for the macroscopic dielectric function but not for phonon frequencies, in contradiction with a claim made in a paper by Arya and Jha. Similar results are obtained for C and Si. This indicates that the extreme-tight-binding band model is too simple to be useful in phonon-dispersion calculations. The present authors have shown elsewhere that the inclusion of the higher bands and the consistency between electron-ion and crystal pseudopotential play an essential role in obtaining meaningful phonon frequencies for semiconductors.

In the extreme-tight-binding model,<sup>1</sup> only one parameter is used in the Hamiltonian matrix, resulting in two flat bands: one valence and one conduction band. Each band is fourfold degenerate. The electron wave functions are Bloch functions of bonding and antibonding states of  $sp^3$  hybridized orbitals centered on neighboring atoms. For each atom  $a$  in the unit cell, four such hybridized orbitals  $\varphi_{ia}(\vec{r})$  can be constructed, each directed towards its nearest neighbor. The orbitals are linear combinations of hydrogenic functions. Since the diamond crystal consists of two interpenetrating fcc lattices, each unit cell has two types of atoms. The bonding states are the wave functions of the valence band and the antibonding states those of the conduction bands. These wave functions are expressed in terms of the orbitals in the following way:

$$\begin{aligned} \Phi_{iv}(\vec{k}, \vec{r}) &= \frac{1}{\sqrt{2N}} \sum_i e^{i\vec{k} \cdot \vec{R}_i} [\varphi_{i1}(\vec{r} - \vec{R}_1) - \varphi_{i2}(\vec{r} - \vec{R}_2 - \vec{\tau}_i)], \\ \Phi_{ic}(\vec{k}, \vec{r}) &= \frac{1}{\sqrt{2N}} \sum_i e^{i\vec{k} \cdot \vec{R}_i} [\varphi_{i1}(\vec{r} - \vec{R}_1) + \varphi_{i2}(\vec{r} - \vec{R}_2 - \vec{\tau}_i)]. \end{aligned} \quad (1)$$

Throughout the present calculation, an origin has been chosen midway between the two atoms of the unit cell, which means that  $\vec{R}_1 = (a/8)(1, 1, 1)$ ,  $\vec{R}_2 = (a/8)(\bar{1}, \bar{1}, \bar{1})$ , and that  $\tau_i$  is a vector from the origin to the  $i$ th neighboring atom of type 2. The direct band gap and the effective charge parameter in the hydrogenic functions of the hybridized orbitals are determined in the same way as Arya and Jha (from here on referred to as Ref. 1) have done earlier, i.e., from the values of the  $(0, 0)$  element of the dielectric matrix and from the requirement that the  $f$ -sum rule is satisfied using only these bonding and antibonding states.

In this model, the dielectric matrix can be written as follows:

$$\begin{aligned} \epsilon(\vec{q}, \vec{G}, \vec{G}') &= \delta_{\vec{G}, \vec{G}'} + \frac{4\pi}{(\vec{q} + \vec{G})^2} \frac{4}{E_g v_c} \sum_{nk} \langle \Phi_{nc} | e^{-i(\vec{q} + \vec{G}) \cdot \vec{r}} | \Phi_{nv} \rangle \\ &\quad \times \langle \Phi_{nv} | e^{i(\vec{q} + \vec{G}') \cdot \vec{r}} | \Phi_{nc} \rangle. \end{aligned} \quad (2)$$

Atomic units are used, i.e.,  $\hbar = m = e = 1$ .

The inversion of the dielectric matrix is achieved by a factorization procedure.<sup>2</sup> For that purpose the polarizability matrix is written as follows:

$$\tilde{\chi}(\vec{q}, \vec{G}, \vec{G}') = \sum_{nm'} N_n^*(\vec{q} + \vec{G}) F_{nm'} N_{n'}(\vec{q} + \vec{G}), \quad (3)$$

where

$$N_n(\vec{q} + \vec{G}) = \langle \Phi_{nv} | e^{i(\vec{q} + \vec{G}) \cdot \vec{r}} | \Phi_{nc} \rangle \quad (4)$$

and

$$F_{nm'} = -\frac{4}{E_g v_c} \delta_{nm'}. \quad (5)$$

Since the orbitals used in the valence and conduction wave functions [Eq. (1)] are linear combinations of hydrogenic functions, the integrals appearing in the function  $N_n$  can be evaluated analytically. Then the inverse dielectric matrix becomes

$$\begin{aligned} \epsilon^{-1}(\vec{q}, \vec{G}, \vec{G}') &= \delta_{\vec{G}, \vec{G}'} + \frac{4\pi}{(\vec{q} + \vec{G})^2} \sum_{nm'} N_n^*(\vec{q} + \vec{G}) A_{nm'} \\ &\quad \times (\vec{q}) N_{n'}(\vec{q} + \vec{G}'), \end{aligned} \quad (6)$$

where

$$A_{nm'}(\vec{q}) = \frac{-4}{E_g v_c} B_{nm'}(\vec{q}) \quad (7)$$

and

$$\begin{aligned} B_{nm'}^{-1}(\vec{q}) &= \delta_{nm'} + \frac{4}{E_g v_c} \sum_{\vec{G}} \frac{4\pi}{(\vec{q} + \vec{G})^2} \\ &\quad \times N_n(\vec{q} + \vec{G}) N_{n'}^*(\vec{q} + \vec{G}). \end{aligned} \quad (8)$$

In this model, the electron-ion part of the dy-

namical matrix takes on the form

$$D_{ij}^{el}(\vec{q}; ab) = \frac{1}{Mv_c} \sum_{nmr} W_n^*(i, a; \vec{q}) A_{nmr}(\vec{q}) W_n(j, b; \vec{q}), \quad (9)$$

where

$$W_n(i, a; \vec{q}) = \sum_{\vec{G}} (\vec{q} + \vec{G})_i V_a(\vec{q} + \vec{G}) e^{-i\vec{G} \cdot \vec{R}_a} N_n(\vec{q} + \vec{G}). \quad (10)$$

$V_a$  is the form factor of the electron-ion pseudopotential. As in Ref. 1 a Shaw pseudopotential is used:

$$V_a(\vec{K}) = -\frac{4\pi Z_a}{K^2} \frac{\sin Kr_c}{Kr_c}, \quad (11)$$

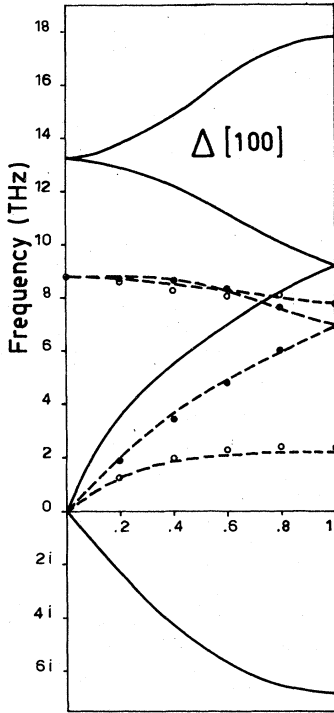


FIG. 1. Phonon dispersion curves for germanium in the  $\Delta$  direction. Dashed line gives results obtained by Arya and Jha (Ref. 1) in the extreme-tight-binding model. Full line refers to calculations in the same model made by the present authors using identical values of the parameters  $a$ ,  $E_g$ , and  $Z_{\text{eff}}$ , as in Ref. 1. However, in the present calculation the product of two electron-ion potentials is used and a summation over as many stars of reciprocal-lattice vectors is performed as needed to obtain convergence. This figure shows clearly that one potential, instead of a product of two, and a lack of convergence will give misleading results. As reported elsewhere (Ref. 8), the effects of the higher bands (neglected in the present calculation) and the consistency between the electron-ion and crystal pseudopotential are essential for obtaining positive squared frequencies. The experimental points are from Nilson and Nelin (Ref. 5).

where  $r_c$  is a parameter. Equation (9) differs from Eq. (13) of Ref. 1 in the electron-ion pseudopotential. Since Eq. (9) is in fact a force-force correlation function, it contains a product of the electron-ion pseudopotential of atom  $a$  and of atom  $b$ . In Ref. 1 only one electron-ion pseudopotential is used.

The acoustic sum rule can be written as follows<sup>3</sup>:

$$\lim_{\vec{q} \rightarrow 0} \sum_{\vec{G}, a} \vec{q} \cdot (\vec{q} + \vec{G}) \chi(\vec{q}, \vec{G}) V_a(\vec{q} + \vec{G}) e^{i\vec{G} \cdot \vec{R}_a} = 0. \quad (12)$$

It should be emphasized that in Ref. 1 the value of the electron-ion pseudopotential parameter  $r_c$  is determined in order to satisfy the acoustic sum rule [Eq. (12)]. In principle this electron-ion potential should be consistent with the total crystal potential, i.e., starting from an atomic electron-ion pseudopotential, the Hartree (or Hartree-Fock) Hamiltonian is solved by iteration until consistency is obtained.<sup>8</sup> However, in this Slater-Koster model the crystal potential is not known explicitly, but the matrix elements of the total Hamiltonian are parametrized and fitted to the experimental values of the electronic band structure. Phenomenologically, one expects that this procedure ensures the choice of a realistic crystal potential. By changing the parameters of the electron-ion potential on top of that, the atomic electron-ion potential is drastically altered and, with that, any control over consistency is lost.

In the present calculation for Ge,<sup>4</sup> the lattice constant  $a$  is 5.647 Å. The band gap  $E_g$  is equal

TABLE I. Dependence of the acoustical sum rule (ASR), in the  $\Gamma$  and  $X$  point for germanium for different values of the parameter  $r_c$  (a.u.). The parameters used in the extreme-tight-binding model are  $a = 5.647$  Å,  $E_g = 3.9$  eV,  $Z_{\text{eff}} = 12.4$ . The bottom line shows the experimental results (Ref. 5). Frequencies are given in  $10^{12}$  Hz.

$r_c$	$10^{-2}$ ASR	TO( $\Gamma$ )	LO( $\Gamma$ )	TO( $X$ )	L( $X$ )	TA( $X$ )
2.2	-0.48	12.29	11.02	17.19	7.70	-8.30
2.0	-0.21	13.44	13.23	18.03	8.97	-6.65
1.8	+0.12	15.69	15.63	19.77	10.41	-4.55
1.7	+0.28	17.02	16.72	20.83	11.06	-3.49
1.6	+0.41	18.26	17.64	21.86	11.60	-2.54
1.5	+0.52	19.31	18.36	22.74	12.02	-1.74
1.4	+0.60	20.09	18.87	23.41	12.32	-1.09
1.3	+0.66	20.64	19.22	23.89	12.52	-0.29
1.2	+0.70	21.09	19.50	24.28	12.67	+0.97
1.1	+0.76	21.63	19.84	24.75	12.87	+1.50
1.0	+0.84	22.51	20.37	25.52	13.17	+1.96
0.9	+0.98	23.98	21.22	26.82	13.66	+2.22
0.8	+1.19	26.22	22.47	28.85	14.38	+1.81
0.7	+1.47	29.35	24.12	31.72	15.32	-2.21
0.6	+1.81	33.30	26.11	35.41	16.43	-4.92
Experiment		9.00	9.00	8.25	6.90	2.45

TABLE II. Dependence of the acoustical sum rule (ASR), in the  $\Gamma$  and  $X$  point for silicon for different values of the parameter  $r_c$  (a.u.). The parameters used in the extreme-tight-binding model are  $a=5.417 \text{ \AA}$ ,  $E_g=5.21 \text{ eV}$ ,  $Z_{\text{eff}}=6.36$ . The bottom line shows the experimental results (Ref. 6). Frequencies are given in  $10^{12}$  Hz.

$r_c$	$10^{-2}$ ASR	TO( $\Gamma$ )	LO( $\Gamma$ )	TO( $X$ )	$L(X)$	TA( $X$ )
1.4	-0.73	61.70	56.63	85.41	40.16	-38.50
1.3	-0.59	63.42	60.22	86.66	40.24	-36.23
1.2	-0.44	65.57	63.82	88.25	40.39	-33.55
1.1	-0.30	68.17	67.43	90.20	40.62	-30.42
1.0	-0.14	71.21	71.04	92.52	40.93	-26.75
0.9	+0.0093	74.55	74.54	95.11	41.24	-22.51
0.8	+0.14	77.72	77.56	97.61	41.42	-17.90
0.7	+0.23	79.86	79.47	99.33	41.24	-13.70
0.6	+0.24	79.97	79.57	99.42	40.48	-12.21
0.5	+0.13	77.44	77.31	97.40	38.95	-15.65
0.4	-0.077	72.64	72.59	93.62	36.51	-22.37
0.3	-0.36	67.08	65.98	89.38	33.22	-29.95
0.2	-0.65	62.68	58.80	86.13	29.50	-36.74
Experiment		15.41	15.41	13.89	12.26	4.55

to 3.9 eV and the effective charge  $Z_{\text{eff}}$  equals 12.4 eV. The values of these parameters are obtained by fitting the  $f$ -sum rule and  $\epsilon(0, 0, 0)$ . The inverse dielectric matrix has been calculated for about 1046 reciprocal-lattice vectors, depending on the star of  $q$ . In Ref. 1 only 40 reciprocal-lattice vectors are used, leaving out the star (311), although in the present calculation it is found that these matrix elements are not zero. With the same value of  $r_c=0.19a$  as in Ref. 1, the calculation yields a value of 17.23 for  $\lim_{q \rightarrow 0} \epsilon(\vec{q}, 0, 0)$  and of 0.9921  $\text{\AA}$  for  $\langle \Phi_{nv} | n | \Phi_{nc} \rangle$ , in agreement with the results of Ref. 1. However, the local field corrections are -10.52, instead of the -1.64 found by Arya and Jha.

The present authors have calculated the phonon

TABLE III. Dependence of the acoustical sum rule (ASR), in the  $\Gamma$  and  $X$  point for diamond for different values of the parameter  $r_c$  (a.u.). The parameters used in the extreme-tight-binding model are  $a=3.560 \text{ \AA}$ ,  $E_g=18.26 \text{ eV}$ ,  $Z_{\text{eff}}=3.16$ . The bottom line shows the experimental results (Ref. 7). Frequencies are given in  $10^{12}$  Hz.

$r_c$	$10^{-2}$ ASR	TO( $\Gamma$ )	LO( $\Gamma$ )	TO( $X$ )	$L(X)$	TA( $X$ )
2.2	-0.45	21.16	19.31	29.54	13.33	-14.08
2.0	-0.25	22.54	22.03	30.54	14.27	-11.87
1.8	+0.020	25.37	25.36	32.68	15.69	-8.60
1.6	+0.29	28.11	28.54	35.66	17.14	-4.64
1.5	+0.41	30.78	29.77	37.05	17.69	-2.28
1.4	+0.49	32.05	30.64	38.11	18.07	+2.27
1.3	+0.53	32.81	31.16	38.75	18.26	+3.36
1.2	+0.56	33.16	31.39	39.04	18.30	+3.84
1.1	+0.57	33.33	31.50	39.19	18.29	+4.15
1.0	+0.59	33.69	31.73	39.49	18.34	+4.52
0.9	+0.64	34.65	32.34	40.31	18.59	+5.09
0.8	+0.77	36.63	33.56	42.03	19.18	+5.71
0.7	+0.95	39.92	35.48	44.93	20.13	+5.92
0.6	+1.22	44.64	38.08	49.16	21.40	+4.75
0.5	+1.53	50.56	41.15	54.59	22.89	-4.17
Experiment		39.93	39.93	32.07	35.52	24.19

frequencies using Eqs. (9) and (10). With the same parameters as above, the dispersion curve in the  $\Delta$  direction for both the present calculation and the one of Ref. 1 is given in Fig. 1. The square of the transverse acoustic modes remains negative for all wave vectors in the  $\Delta$  direction. This result is in complete disagreement with the curves obtained by the authors of Ref. 1. However, it should be emphasized that in the present calculation the product of two electron-ion potentials, instead of one potential, and summations over as many reciprocal-lattice vectors as needed to obtain convergence, are used. As can be seen from Table I, it is possible to obtain positive modes at the  $X$  point for values of the parameter  $r_c$  of the

TABLE IV. Convergence of the macroscopic dielectric function  $\epsilon_m$  and the phonon frequencies at the  $\Gamma$  and  $X$  point with respect to the number of reciprocal-lattice vectors used in the dielectric matrix. Results given for germanium with  $E_g=3.9 \text{ eV}$ ,  $Z_{\text{eff}}=12.4$ , and  $r_c=2.0276$  a.u.

No. vectors $\Gamma$	$\epsilon_m(\Gamma)$	$10^{-2}$ ASR	TO( $\Gamma$ )	No. vectors $X$	$\epsilon_m(X)$	TO( $X$ )	$L(X)$	TA( $X$ )
15	7.8496	0.1095	15.20	14	3.5997	19.37	9.98	-1.83
27	7.1713	-0.0958	13.93	40	3.1146	18.39	8.53	-5.23
97	6.8174	-0.3155	12.83	92	3.0932	17.59	7.44	-7.43
169	6.7831	-0.2615	13.12	190	3.0749	17.79	7.74	-6.96
267	6.7816	-0.2696	13.09	254	3.0579	17.76	7.92	-7.02
339	6.7767	-0.2759	13.05	388	3.0339	17.74	7.96	-7.06
531	6.7482	-0.2813	13.03	468	3.0255	17.73	7.93	-7.09
1046	6.7143	-0.2852	13.0282	1034	3.0147	17.7265	7.9300	-7.0970
2927	6.7038	-0.2864	13.0265	2954	3.0093	17.7253	7.9319	-7.0999

